Development of In-Flow Phased Microphone Array Windscreen Corrections for Small and Large Arrays

Nathan J. Burnside[1] and William C. Horne[2]
NASA Ames Research Center, Moffett Field, CA 94035

The corrections needed in acoustic level measurements using an in-flow phased-array were documented with detailed measurements in the NASA Ames 25- by 18- by 11-Ft Anechoic Chamber for 4 different in-flow arrays fitted with conformal windscreens of stainless-steel wire cloth and Kevlar120 fabric. This study considered the effects of source measurement angle and distance, and the effects of compact vs large distributed broadband calibration-sources. The study verified a simple geometric scaling that accurately derives the windscreen correction for arbitrary incidence angles from the correction measured at normal incidence. The acoustic corrections for windscreens of stainless-steel wire cloth with 200x600 wires/inch were significantly smaller and more regular than for the Kevlar120 windscreen. The qualitative effects of screen tautness were measured and found to be insignificant for the typical assembly specifications at Ames. Correcting phased array peak levels with the measured windscreen corrections created results that compare well with free-field microphone measurements of broadband noise sources.

I. Nomenclature

θe	=	source emission angle, degrees
C_{WS}	=	windscreen correction, dB
f	=	frequency, Hz
Kevlar120	=	Kevlar screen material, 1.8 oz/yard, 34x34 strands/inch, open weave
ss200x600	=	stainless-steel screen material, 200x600 wires/inch, dutch twill weave

II. Background and Objectives

Phased microphone arrays are powerful tools for measuring both the levels and locations of a variety of airframe and propulsion related noise sources in open- and closed test section wind tunnels [1, 2]. In addition, the design of the array [3-5] and processing algorithms [6, 7] can be optimized to maximize measurement resolution and accuracy while minimizing the interference from facility wall reflections, drive noise, and turbulent flow noise over the surface of in-flow sensors. In practice, the application of microphone arrays to acquire measurements from a wind tunnel aeroacoustic study will generally require practical procedures for calibrating the array sensors with known reference sources and for estimating the overall measurement accuracy of the study results.

Studies of in- and out-of-flow array measurements of reference acoustic sources in closed- and open-test section wind tunnels (and anechoic chambers) have been previously reported [8-10]. These studies focused primarily on quantifying the effects of porous windscreens on the suppression of background noise from the turbulent boundary layer over in-flow arrays. Contrary to the suppression of flow noise is the modification of the array acoustic response due to windscreens of various materials and the associated cavity between the screen and the array plate.

In-flow phased arrays are placed within the flow stream of wind tunnels to determine levels and locations of acoustic sources radiating from research test models. Pressure fluctuations from the boundary layer on the array surface created by the wind-tunnel stream can significantly mask the acoustic radiation arriving from the model. In

[1] Aerospace Engineer, Senior Member AIAA
[2] Retired Aerospace Engineer, Associate Fellow AIAA

order to attenuate the boundary layer noise, the microphones are recessed in a cavity and a stainless-steel or a Kevlar screen is placed flush on the top surface of the array. While such screens greatly help with the attenuation of the boundary layer noise, they also create a semi-reverberant cavity on top of the microphone sensors that can selectively attenuate or even amplify the incoming sound waves. The goal of this paper is to determine the correction factors necessary to account for the cavity reverberation of four different phased arrays for use in future tests.

Horne et al. [9] quantified the reduction of turbulent flow noise for a screen-covered in-flow array as a function of screen material and resistance to steady flow through the screen. Stainless-steel cloth with 200x600 wires/inch and a normal flow resistance of 80 MKS Rayls was found to be a suitable compromise between suppression of turbulent flow noise and minimal alteration of acoustic response. For this material, and a cavity depth of 0.5 inches, the response to a compact source normal to the array plate was modified by 1/4-wave resonances that attenuated the bare plate response an average of 1 to 1.5 dB with peak variations of about 1.5 dB over a 100 kHz range for an 8-inch diameter array. The measured normal response was found to correspond well to a simple acoustic model of massless and acoustically resistive screen suspended over a rigid plate.

The response to sources at other directions from normal were reported first by Fleury [5], who found that the resonant peak frequencies increased as $1/\sin(\theta e)$ relative to the normal response resonant peak frequencies at $\theta e = 90^{o}$. The effective cavity depth seen by a sound wave incident at an off-normal direction increases by the above factor. Horne et al. [9] also found that the resonant peak amplitudes diminished as $\sin(\theta e)$. These effects will be discussed in more detail in the results section.

The goal of the present study is to build on the previous results to develop a practical approach for calibrating in-flow microphone arrays with windscreens and to quantify the accuracy of resulting measurements from wind tunnel research studies. This investigation will address the effects of array size, windscreen material, calibration source size and configuration, and the angle and distance from the array to the calibration source. The results of the present study were obtained in an anechoic chamber with no freestream effects. A brief discussion on application of these results for calibration and measurement corrections in a wind tunnel with freestream velocity is included in the appendix, based on results from previous wind tunnel studies.

A. Test Hardware and Experimental Setup

Tests were conducted at the NASA ARC anechoic chamber using pneumatic broadband noise sources mounted at the far end of the chamber. The chamber is 18 feet wide by 25 feet long by 11 feet high and its walls are covered by 18 inches deep fiberglass wedges; the chamber is anechoic down to 250 Hz.

Three planar arrays were evaluated in this study, with pattern diameters of 8, 23, and 32 inches. Each array was mounted atop a motor driven turntable on a pedestal which rode on a set of linear rails with a manual traversing carriage. Figure 1 shows the back of the 32-inch array in the 4-foot calibration position with an incidence angle of about 80 degrees. A G.R.A.S. ¼-inch condenser microphone was mounted to the traversing carriage without an array to measure the free-field acoustic environment at each of the 3 calibration distances: 4, 8, and 16 feet.

The primary calibration noise source for this study was the airball developed at NASA Ames. The airball is a 2-inch diameter stainless-steel sphere with 44 micro-jets drilled into the outward facing hemisphere. This sphere was installed within an aerodynamic fairing with total temperature and total pressure sensors as shown in Figure 2. The airball was supplied with low-pressure shop air and has been documented in previous studies [8, 12]. To look at the effects of a distributed source on the windscreen corrections, another pneumatic source with a linear array of regularly spaced holes was used as shown in Figure 3. The micro-jets impinged on a screen to increase the low frequency acoustic energy.

Using the same 200x600 wire/inch stainless-steel windscreen that Horne et al. tested in 2020 [9], a total of nine large diameter windscreens were fabricated for use in closed-wall test sections. Five of the 32-inch diameter arrays were used in previous studies with Kevlar windscreens that attenuated boundary layer noise but introduced reverberations that were higher in amplitude than the stainless-steel screen. The in-flow Kevlar screen also introduced broadband scrubbing noise above 15 kHz. One of the new screens was the primary focus of this study, it was calibrated while installed on two large diameter arrays. The 32-inch diameter array with a Kevlar120 windscreen was also calibrated in this study to compare with a previous study by Horne and Burnside [12].

Four array patterns were included in this study to verify previous small-diameter array results and to measure the new ss200x600 large-diameter screen corrections. The majority of the previous windscreen correction data were developed and optimized for the 8-inch diameter array which has 24 condenser microphones in a 3 spiral-arm pattern referred to as the Common Array (CA) because three identical arrays are available for use at NASA Ames, Glenn, and Langley [8, 9]. Figure 4 shows the array pattern used and its installation into the custom built in-flow array fairing.

Windscreen corrections were also developed using two larger diameter array patterns, both with unique characteristics. First, a 24-element array with a 32-inch diameter pattern using lower cost electret microphones

designed for measurements in the frequency range of 0.2 to 20 kHz was calibrated with the ss200x600 windscreen. Development of this array and its anticipated uses were previously documented [4] and is referred to as the wall array because it was designed to mount into the wall or floor of the AEDC 40x80 Foot Wind Tunnel. The second large diameter array studied has a 49-element condenser microphone pattern with a diameter of 23 inches, that contains two nested, coaxial patterns of 24 elements and a center microphone, first reported by Horne and Burnside [12]. The inner 8-inch array and outer 23-inch array are referred to as I24 and O24, respectively. A summary of the arrays is shown below Table 1.

Table 1 Summary of arrays tested and presented here.

Name	Diameter	# Microphones	Type	Comment
Wall Array	32 inches	24	electret	low cost, <20kHz
I24	8 inches	24	condenser	co-axial with O24, <75 khz
O24	23 inches	24	condenser	co-axial with I24, < 75 kHz
Common Array	8 inches	24	condenser	

III. Results

A. Wall Array (32-inch, 24 electret microphones)

Windscreen correction factors, $C_{WS}(\theta e,f)$, are a function of frequency and source emission angle:

$$C_{WS}(\theta_e, f) = Lp(no\ screen) - Lp(with\ screen), \text{[dB]}. \quad (1)$$

Correction factors were calculated by measuring the noise source with and without the screens at each incidence angle, θ_e. Conventional beamforming contour maps were created for each measurement and the difference in peak beamformed levels between no screen and screen is the correction factor, C_{WS}. The measurements were repeated for three different separation distances between the array and the noise source.

Figure 5 shows the contour maps of C_{WS} for the ss200x600 screen and the wall array measured at 3 different distances. Note that a positive value of C_{WS} implies damping of the incident acoustic waves and a negative value is an amplification. Although the wall array is typically used for a source frequency range of 0.2 to 20 kHz, the measurements were made to include the frequency response of the electret microphones (30 kHz). Figure 5b and Figure 5c, the 8 foot and 16-foot distances, have similar patterns showing about a 2.8 dB correction at 20 kHz and 27 kHz for 90-degree emission. Figure 5a shows a different contour pattern but it should be noted that this 32-inch array was not designed for use with a 4-foot source to array spacing. Figure 5d plots the 16-foot distance for the broadside condition for clarity. It is apparent from the results that limiting the use of the wall array to 20 kHz and below would likely reduce or eliminate the need for screen correction factors.

Fleury [5] developed a useful extrapolation of the windscreen correction from the measured correction spectrum at 90˚ incidence angle:

$$C_{WS}(\theta_e, f) = C_{WS}\left(90°, f * sin(\theta_e)\right), \text{[dB]}. \quad (2)$$

Horne et al. [9]. extended this extrapolation to include a sin(θe) coefficient to create decay at incidence angles other than 90º as the measured results indicate:

$$C_{WS}(\theta_e, f) = \sin(\theta_e) * C_{WS}(90°, f * sin(\theta_e)), \text{[dB]}. \quad (3)$$

Making calibration measurements at only one incidence angle, makes application of screen corrections less cumbersome and allots the researcher the attention to make precise measurements of a single angle instead of a wide range of incidence angles. Aside from the simplicity and convenience, the correction contours are smoother and closely resemble the measured corrections but with less scatter from low angular resolution.

Figure 6 presents the s200x600 screen correction using equation 3 and a cubic spline fit of the measured 90º 1/12th-octave spectrum. Most of the corrections are limited to less than 2 dB except for a peak at 18 kHz at the 16-foot distance. While data were acquired at 37 incidence angles for each array only screen corrections factors calculated using equation 3 (Fleury-Horne method) will be presented for the remainder of this paper. The 90º correction curve of Figure 6d shows three correction peaks at 5, 17, and 30 kHz correction with an overall range of -0.8 to + 3dB. This is also the range of measurement accuracy if corrections were not applied.

Figure 7 shows the same measurements for the Kevlar120 screen which produces much more dramatic windscreen corrections. Figure 7a to Figure 7d show corrections ranging from about -1 to 5 dB over all distances and with strong incidence angle dependance. At frequencies as low as 10 kHz corrections of 3 dB are necessary for the Kevlar screen. The correction peak frequencies are at 12 and 24 kHz. It is apparent that ss200x600 is a more suitable windscreen material to limit the severity of data corrections needed which is consistent with the results reported by Horne and Burnside [12]. Previous wind tunnel studies, including [9] have noted turbulent flow scrubbing noise at about 15 kHz that is not observed with the stainless-steel screen.

B. I24 and O24 (23-inch, coaxial, condenser microphones)

Windscreen corrections were calculated for the 49-element condenser array with nested patterns I24 (8-inch diameter) and O24 (23-inch diameter) to 95 kHz using the Equation 3 for the ss200x600 windscreen. These arrays have the same relative array pattern as the wall array with an additional microphone at the array center. Figure 8a to Figure 8c show symmetric, repeating correction contours with similar amplitudes for the smaller 8-inch I24 array. Corrections range from 0 to 3 dB over the full frequency and incidence angle range. Figure 8d shows a regular reverberation pattern with 8 regularly spaced peaks and with correction amplitude increasing slightly with frequency.

Figure 9 presents the 23-inch O24 corrections for the ss200x600 screen in the same format as the smaller I24 pattern. Very similar to the I24 pattern, O24 shows a 0 to 3 dB correction over the full frequency and incidence angle ranges. However, at the 16-foot propagation distance, the lower peaks of the correction skew away from 0 dB towards 1 dB.

To explore the difference between the 8-inch and 23-inch pattern, Figure 10 presents the 90˚ results for each array at 4, 8, and 16 feet. Keep in mind that the 23-inch pattern is a scaled version of the 8-inch pattern and that the data for both patterns were acquired simultaneously. In general, the peaks of the corrections range from 2 to 3 dB for both arrays except the O24 has more scatter and the local minima increase with frequency. Horne and Burnside [8] showed a decreasing coherence between the center microphone of an array and the outer microphone with increasing frequency. It is intuitive that coherence would decrease more rapidly for a larger diameter array which could explain the variations at higher frequencies for the O24 array. Edge effects could also cause the higher frequency variations. The nested 49-element pattern has the same diameter ss200x600 windscreen and the O24 array has its outer most microphones much closer to the edge of the screen than I24.

C. Airball vs Linear Source

This study used two different noise sources, a compact airball and a linear array of micro-jets to calibrate the ss200x600 windscreen using the 49-element nested I24 and O24 arrays. Windscreen corrections derived from the different sources proved to be similar as shown in Figure 11. Figure 11a presents the compact airball results and Figure 11b presents the linear source; both have similar amplitudes and frequency patterns. Results for different distances and the O24 pattern were similar to the 90˚ correction as shown in Figure 11c.

D. Common Array

A previous study by Horne et al. [9] included extensive research on the ss200x600 for the 8-inch Common Array (CA), which was the basis for extending the ss200x600 screen to larger diameter arrays. Measurements from the 2020 screen calibrations were repeated here in 2022 and the comparison is shown in Figure 12. There are subtle differences but the overall amplitude and shape of the C_{WS} contours are the same. The similarities in the measurements made using two different experimental setups, two years apart, gives confidence in the windscreen correction method presented in equation 3. Many of the 90º correction plots have correction peaks with little variation in minimum and maximum peak levels over the frequency range, as in Figure 10c. Other 90º corrections exhibit a small but noticeable ramp of these levels with frequency, as in Figure 9d. The causes of these variations are not fully understood but will be explored further with the results of these studies.

E. Common Array Tension Study

One variable that has not been explored thus far is the tension of the windscreen. When attaching windscreens, researchers at NASA Ames have always taken care to tighten the screen in an alternating pattern as opposed to tightening screws circumferentially to apply an even tension to the screen. The screens are tightened so that they are taught, and the edge of the screen is as flush with the mounting plate as possible. However, a quantitative measurement of screen tension has not been applied. One would have to measure the screen displacement under a given force to accurately measure the tension. To qualitatively access the importance of screen tension, measurements were made with the Common Array with the screen tight, loose, and very loose. Results are presented in Figure 13 showing that reverberation and therefore C_{WS} decreases with decreasing tension as frequency increases. The installation procedures

at NASA Ames have always resulted in a tight screen and therefore tension is assumed to not affect the screen corrections.

F. Application of C_{WS} to Data

Applying the derived windscreen corrections to the peak array levels of each array at various incidence angles and over a range of distances while comparing to measurements made with a free-field microphone allows one to access the overall quality and accuracy of the microphone arrays. Amplitudes were corrected for source pressure variation and the effects of using a free-field microphone embedded in a flat plate. Results for the 32-inch electret array are shown in Figure 14a to Figure 14c. For incidence angles between 60˚ and 120˚ array peak levels are accurate to within 1 dB up to 18 kHz and distances greater than 4 feet. It was expected that the 32-inch array would perform poorly at 4 feet due to very large capture angle. Incidence angles outside of the 60˚ to 120˚ range are accurate to 2 kHz and then drop by about 5 dB for all distances; notice the falloff of array microphone response after about 18 kHz.

The 49-element nested array extends the useful frequency range to about 80 kHz as indicated by the results in Figure 15 for the smaller 8-inch I24 array. Here I24 array peak levels are accurate up to 10kHz for all distances and incidence angles between 30˚ and 150˚. Above 10 kHz the amplitude of incidence angles between 60˚ and 120˚ has decreasing accuracy at shorter distances. The more extreme angles of 30˚ and 150˚ have between 5 dB and 10 dB fall off above 10 kHz.

Finally, Figure 16 presents the results for the O24 nested array in the same fashion. For all angles and distances below 2 kHz O24 peak levels are accurate to within 1dB. As with I24, accuracy decreases with extreme incidence angles and closer distances. The results presented here combine the effectiveness of windscreen corrections with the tradeoffs of array design. Level accuracy is improved by using smaller diameter arrays or by reducing the included angle by increasing source to array distance.

The results presented here were acquired in an anechoic chamber with static air, however the windscreen corrections apply to arrays placed into wind tunnels. The incident angle of the incoming wave is affected by the boundary layer above the wind screen and freestream convected angles must be used. Horne et al. [9] documented the steps necessary to apply static windscreen corrections to data acquired with a freestream velocity. A brief summary of the methods is included in the appendix of this paper.

IV. Conclusions

The effects of Kevlar and stainless-steel cloth windscreens on the acoustic response of three planar arrays have been measured in the NASA Ames anechoic chamber using a broadband pneumatic sources. The array pattern diameters were 8, 23, and 32 inches. The arrays were positioned at a range of distances and incidence angles relative to the fixed source. Conclusions from this study include:

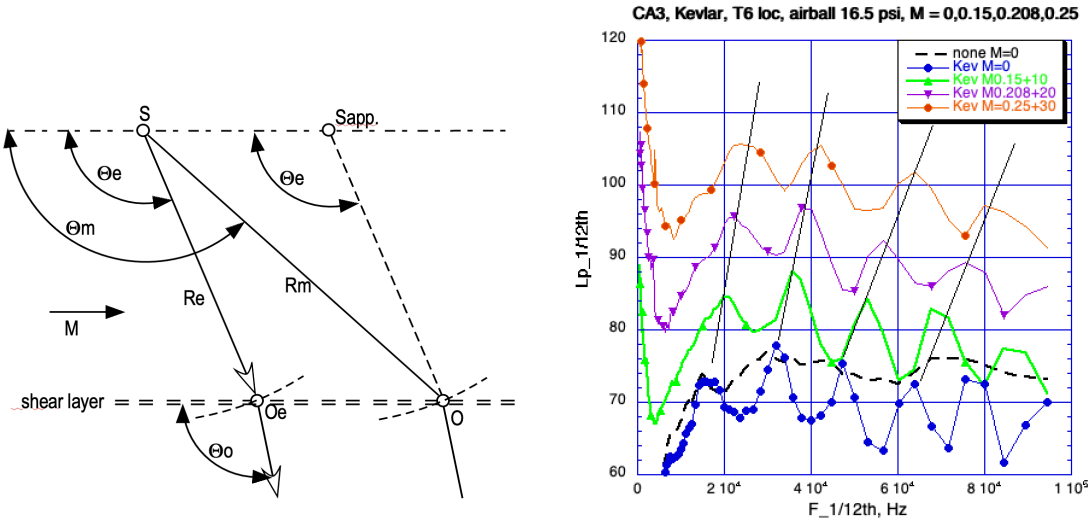
- The simple screen correction method proposed by Horne et al. [9] which uses the C_{WS} measured at 90 deg incidence extrapolated to the full range of incidence angles corresponds well to measurements of C_{WS} over the full angular range.
- Stainless-steel 200x600 screen material proves to require lower screen corrections than Kevlar120 for array patterns ranging from 8 inches to 32 inches.
- Windscreen corrections appear to be largely independent of array diameter assuming one accounts for edge effects.
- Distance has little influence on windscreen corrections assuming one uses an appropriate diameter array.
- Windscreen corrections derived from linearly spaced microjets in a tubular, 18 inch, distributed source are similar to those produced with a compact airball noise source.
- Array screen tension influences windscreen corrections but only when the screens are grossly under tensioned.
- Applying windscreen corrections derived here to measured data produces accurate peak levels given an appropriately sized array and measurement distance.

The results of this study are being incorporated into ongoing research studies at NASA Ames.

Appendix

A. Application of static calibration and correction methods to arrays for wind tunnel studies

The results of the anechoic chamber calibration results correspond well with similar wind-off calibrations of the same array in a hard-wall wind tunnel [8, 9]. Horne et al also conducted a wind-on calibration with a movable source fairing [9] at 3 Mach numbers up to 0.25. In that test, the angle to the source from the array needed to be corrected for convection effects, using the procedure reported by Soderman and Allen [13]. An illustration of the convection effect for a Kevlar windscreen on the 8 in. diam array at various Mach numbers is shown in Ref 9 Figures 14 and 15, reproduced below:



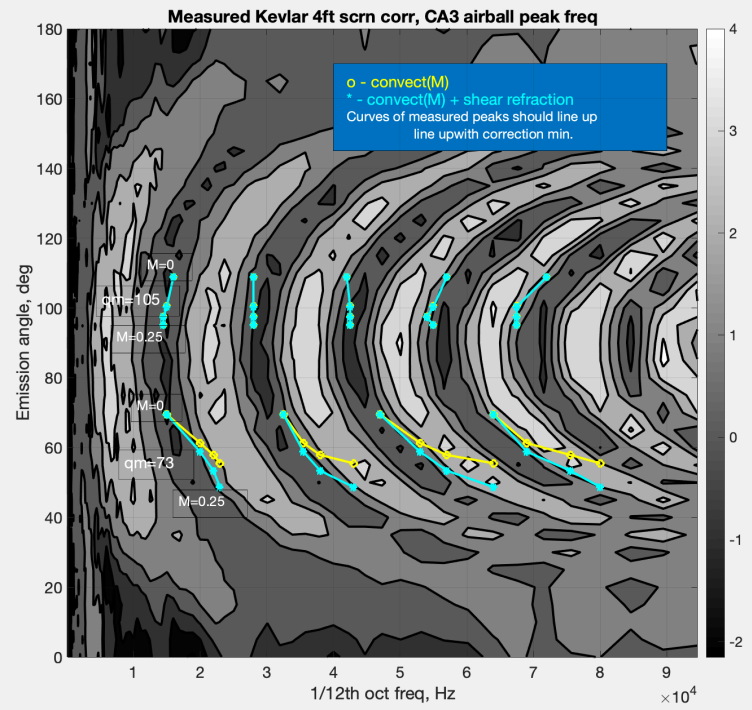
Ref 9 Figure 14 (left), measurement geometry with convection, Ref 9 Figure 15 (right), effects of convection on uncorrected array response to airball source at θm = 73.4º

Note that the frequencies of the response peaks shift higher with Mach number increasing from 0 (lowest 2 curves) to M = 0.15, 0.208, and 0.25 for the increasingly higher curves. Increments of 10 dB were added to each of the non-zero Mach number curves for visibility.

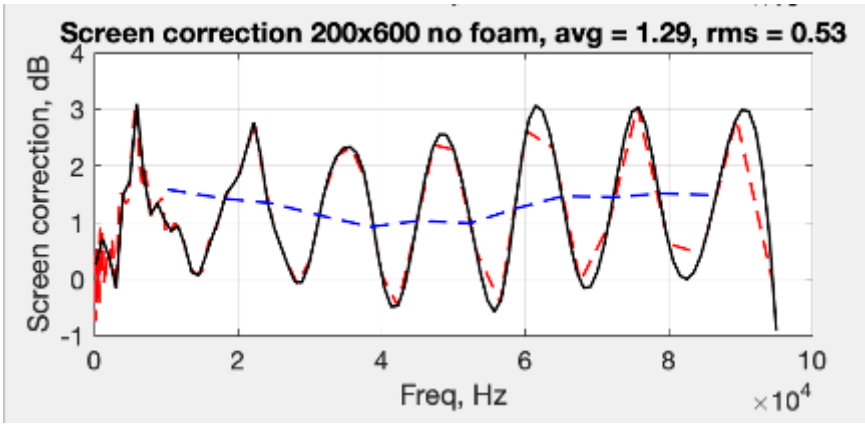
Ref 9 Figure 16 below, shows that this behavior fits well to the static wind screen correction (M=0) if the peak frequencies are plotted against convected emission angle θe for various M. The agreement between the measured peak frequency and the shape of the correction minima improves when refraction at the windscreen θo is also accounted for (yellow lines). For this plot, the frequency peaks of Ref 9 Figure 15 appear as the lower sets of data in Ref 9 Figure 16. Additional measurements of response peak frequencies from the calibration source near 90º showed smaller variation with frequency as seen in the upper set of blue lines for θm ~ 110º.

Although the response frequency peaks for the compact airball source compare well with the minima of the static correction map (darkest greyscales), the correction scheme for this array is complex can be sensitive to small errors in source location. The correction scheme would be considerably more complex for a large distributed source, where a distribution of sub-source locations will each require different convection corrections. Ref 9 Figure 16 shows that small differences in source angle can lead to large errors in the correction value. Ideally the measured peaks should overlap the troughs of the correction map (darkest grey) but this was not generally the case. This issue would not be as severe for the larger electret array that exhibit only 2 or 3 peaks in the 90º Cws graph of this paper Figure 6d.

A modified correction scheme for the arrays and windscreens of this report would be to develop a smoothed correction map extrapolated from the 90º correction graph. The modified correction, Cws_avg, can be computed as a running average of the minimum and maximum peaks, as shown in the plot for ss200x600 reproduced from Ref 9 Figure 11. This would adjust the measurements for the average correction only, the uncorrected ripples in the measurements would introduce errors of +/- 1 dB but greatly simplify the convection corrections for the array and would not affect the computation of overall levels or n-octave bands that average multiple peaks.



Ref 9 Fig. 16 Wind tunnel measurements uncorrected array (with Kevlar screen) response to the airball source in 7x10 ft wind tunnel. Plots of array spectra peak frequencies for M = 0, 0.15, 0.208, and 0.25 corrected for convection only (yellow line) and convection plus shear layer refraction (cyan line) for θm = 105.3° (upper lines) and 73.4° (lower lines). The lines of peak response frequencies are superposed on the anechoic chamber.



Ref 9 Fig. 11, 90° screen correction Cws for ss200x600. Measured 12th octave correction (red dash), cubic spline fit (solid black), and running average between maxima and minima in Cws (dash blue).

Acknowledgments

This study was supported by NASA's Aeronautical Research Mission Directorate (ARMD) Advanced Air Transport Technology Project (AATT). The authors would like to thank Mr. Aksay Naik for his help in data acquisition and Mr. David Keil for fabrication and machining support.

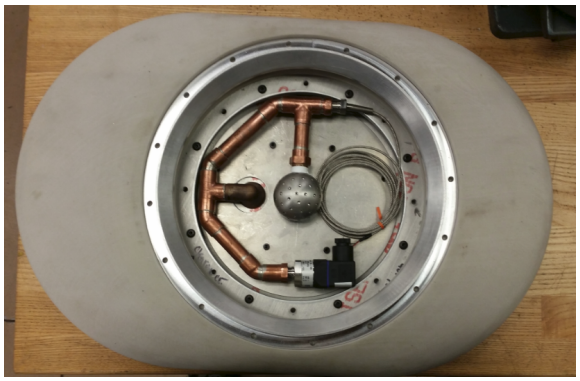
References

1. Underbrink, J., "Aeroacoustic Phased Array Testing in Low Speed Wind Tunnels", in Aeroacoustic Measurements, T. Mueller, ed., Springer 2002.
2. Dougherty, R., "Beamforming in Acoustic Testing", in Aeroacoustic Measurements, T. Mueller, ed., Springer, 2002, p. 93.
3. Jaeger, S., Horne, W., and Allen, C., "Effect of Surface Treatment on Array Microphone Self Noise", AIAA-2000-1937, 6th AIAA/CEAS Aeroacoustics Conf. and Exhibit, 12-14 2000, Lahaina, HI.
4. Horne, W., and Burnside, N., "Development of New Wall-mounted and Strut-mounted Phased Microphone Arrays for Acoustic Measurements in Closed Test-section Wind Tunnels", AIAA 2015-2975, 21st AIAA/CEAS Aeroacoustics Conference, June 22-26 2015, Dallas, TX.
5. Fleury, V., "Optimization of Microphone Array Wall Mountings in Closed-Section Wind Tunnels", AIAA Journal, v. 50, no. 11, Nov. 2012.
6. Bahr, C., and Horne, W., "Advanced Background Noise Subtraction Applied to Aeroacoustic Wind Tunnel Testing", AIAA-2015-3272, AIAA Aviation Forum/AIAA 21st Aeroacoustics Conference, 22-26 June, 2015, Dallas, TX.
7. Dougherty, R., "Functional Beamforming Linear Programming for Determining Aeroacoustic Component Spectra", AIAA-2022-2853, 28th AIAA/CEAS Aeroacoustics Conference, 14-17 June, 2022, Southampton, UK.
8. Horne, W., and Burnside, N., "Initial Calibrations and Wind Tunnel Test Results for an In-Flow Reference Array using New In-Flow Acoustic Sources in Four Array Mount Configurations", AIAA-2018-2969, 2018AIAA/CEAS Aeroacoustics Conf., 25-29 June 2018, Atlanta, GA.
9. Horne, W.C., Burnside, N.J., Schery, S.D., Podboy, G.G., Bahr, C.J., Stead, D.J., Humphreys, W.M., "Effects of resistive windscreens and foam inserts on the acoustic response of an in-flow phased microphone array", AIAA 2021-0217, AIAA SciTech 2021 Forum, 11-15 & 19-21 January 2021, Virtual Event.
10. Szöke, M., and Azarpeyvand, M, "Reduction of the Hydrodynamic Noise on a Beamforming Array", BeBeC-2016-D2, 7th Berlin Beamforming Conference, 29 Feb. – 1 Mar, 2016, Berlin, Germany.
11. Soderman, P., and Allen, C., "Microphone Measurements In and Out of Airstream", in Aeroacoustic Measurements, T. Mueller, ed., Springer, 2002, p. 32 and 36.
12. Horne, W., and Burnside, N., "Measurements of the Effects of Array Pattern Size and Windscreen Material on the Performance of a Wall-mounted Phased Microphone Array in a Hard-wall Wind Tunnel Using Enhanced In-flow Reference Sources", AIAA-2019-2411, 25th AIAA/CEAS Aeroacoustics Conf., Delft, NL, 20-23 May 2019.
13. Dougherty, R., "Directional Acoustic Attenuation of Planar Foam Rubber Windscreens for Phased Arrays", BeBeC-2012-0, Berlin Beamforming Conference, 2012.

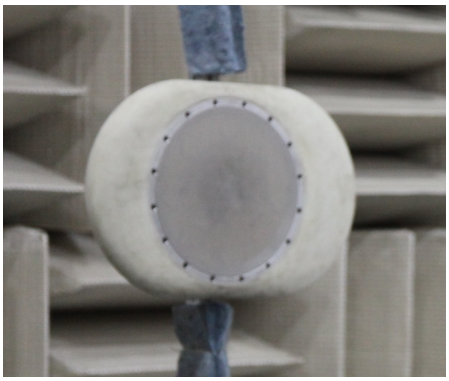
Figures



Figure 1 Windscreen calibration of 32-inch diameter array in the anechoic chamber. The front of the array is facing the calibration noise source fairing at the 4-foot distance.



a) airball has 44 microjets

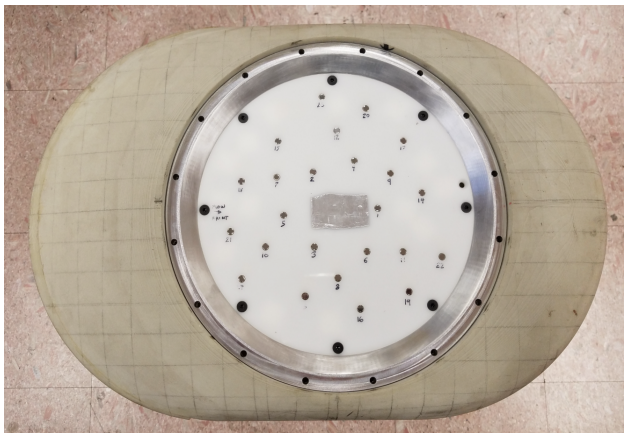


b) airball with windscreen installed

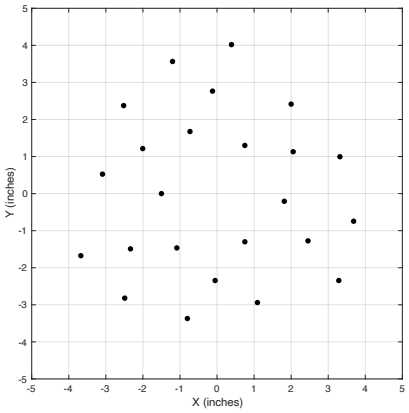
Figure 2 The airball serves as an inflow acoustic calibration device. Notice the total temperature probe and total pressure sensor are in close proximity to the airball.



Figure 3 Linear air source installed in anechoic chamber.

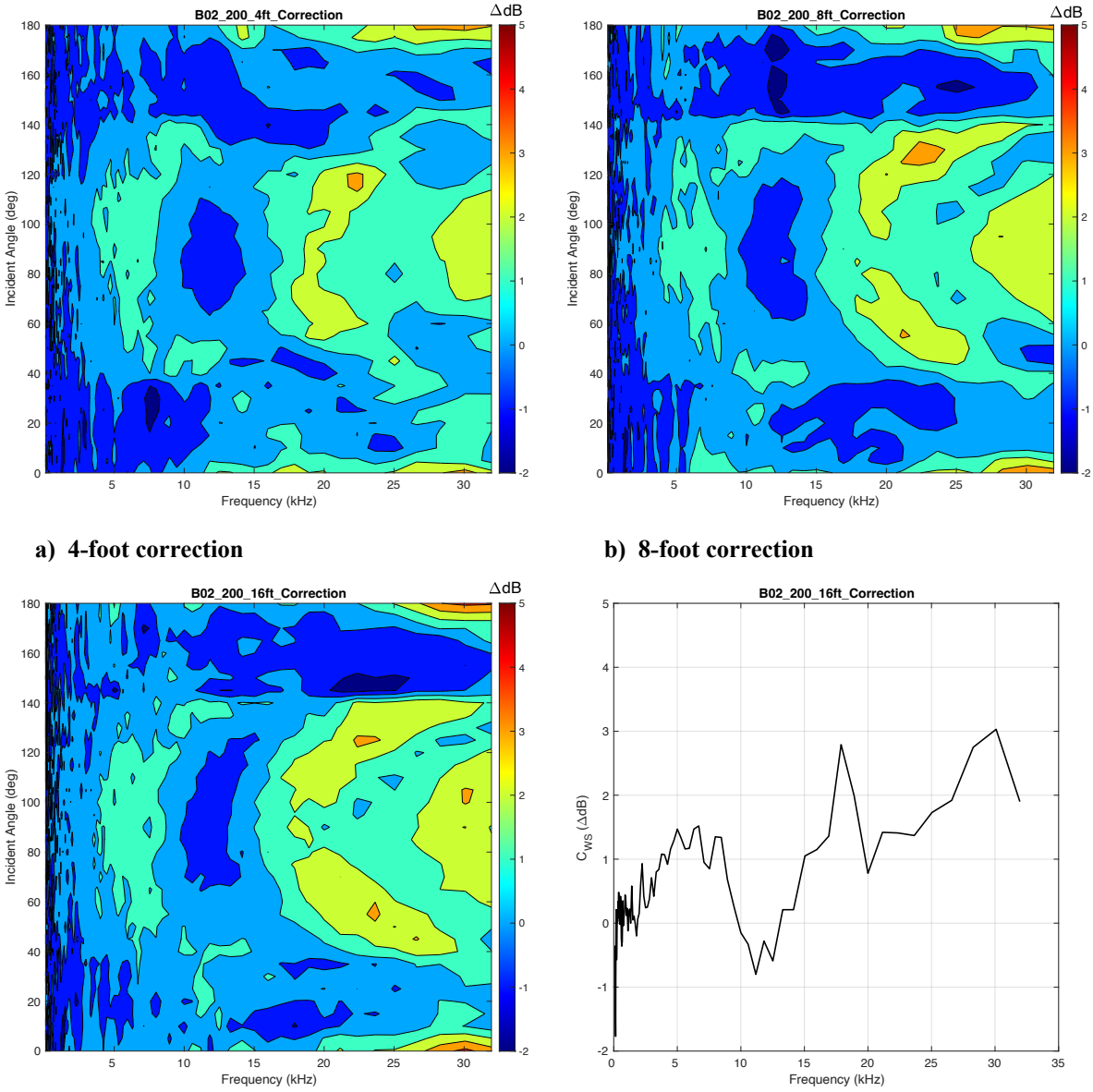


a) ARC array in fairing



b) Array pattern

Figure 4 The common array uses a 24-element 8-inch pattern with condenser microphones.



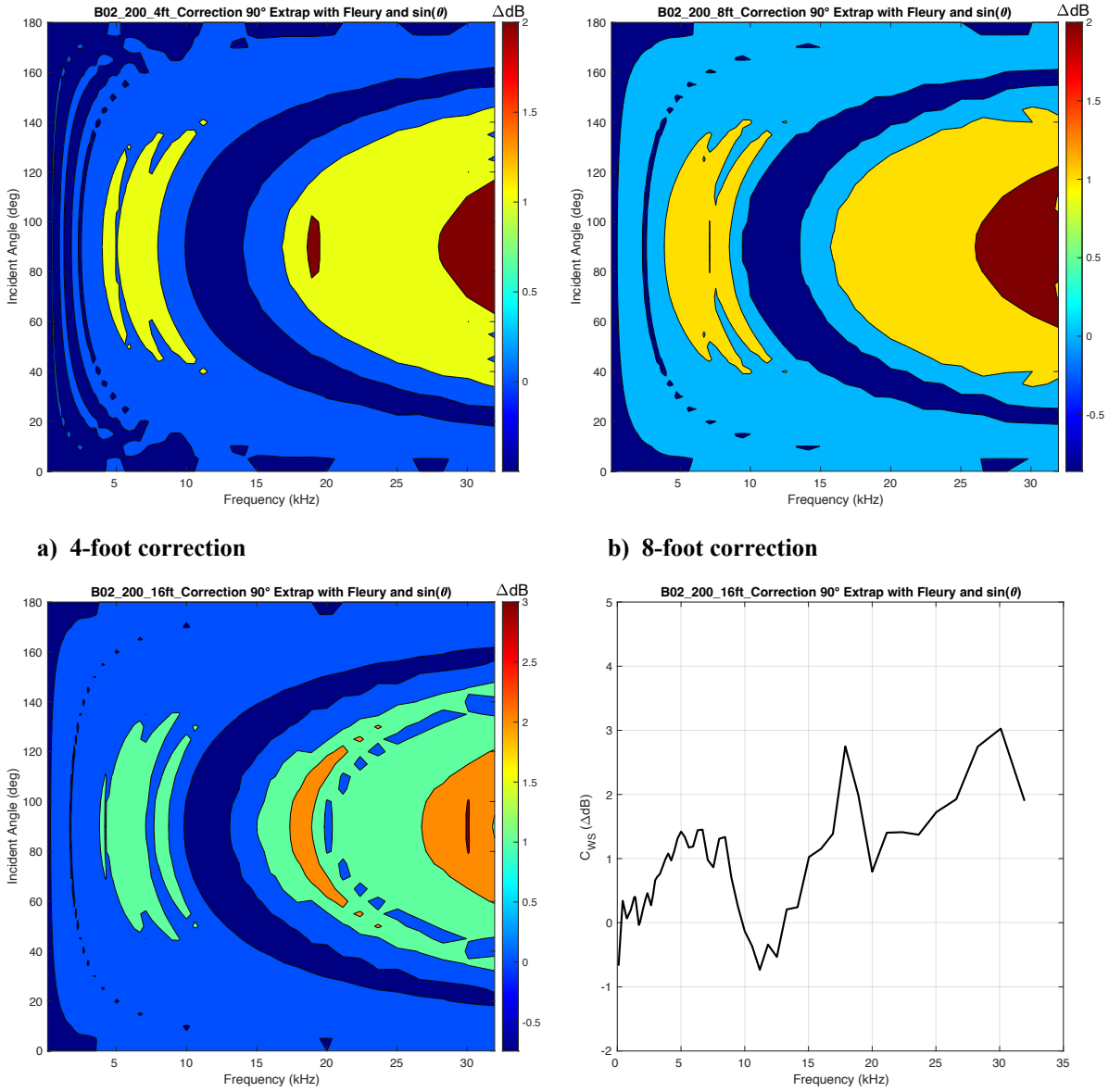
a) 4-foot correction

b) 8-foot correction

c) 16-foot correction

d) 90˚ correction at 16 feet

Figure 5 Windscreen corrections using airball source for the ss200x600 screen and the 32-inch electret array.



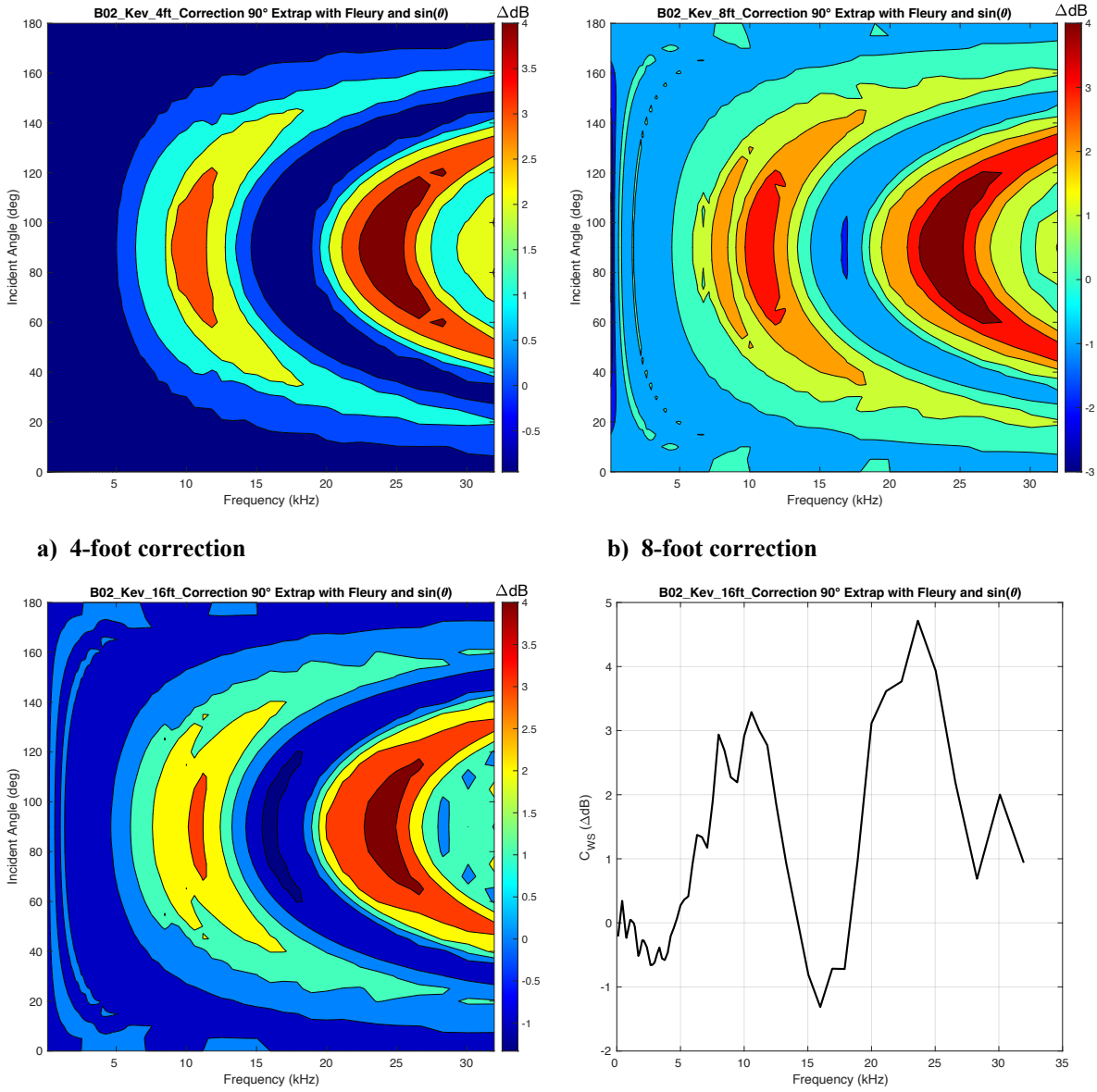
a) 4-foot correction

b) 8-foot correction

c) 16-foot correction

d) 90˚ correction at 16 feet

Figure 6 Windscreen correction for 32-inch electret array with ss200x600 extrapolated from 90˚ measurements using the Fleury method and sin(θe) amplitude modifier (Fleury-Horne method).



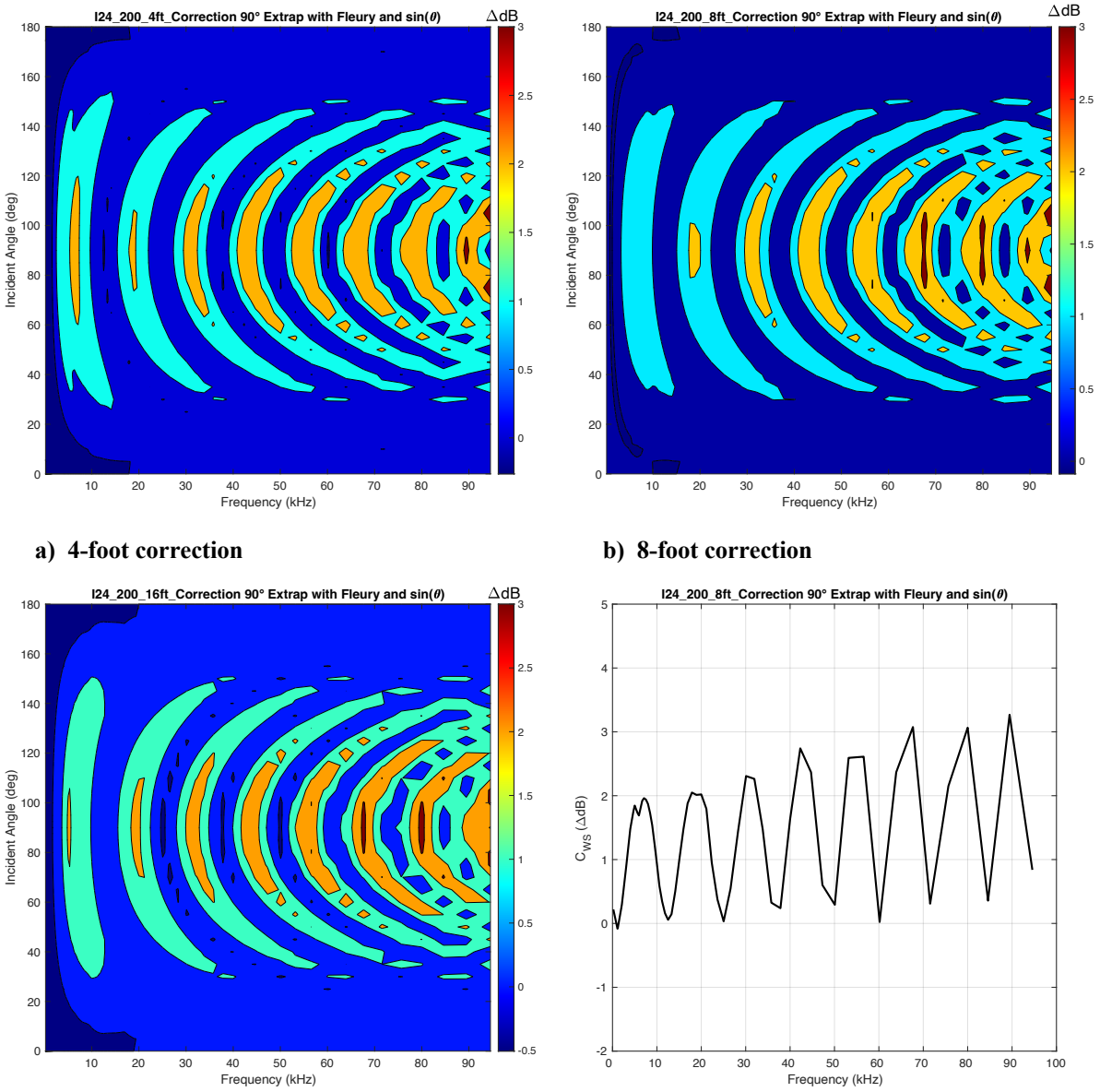
a) 4-foot correction

b) 8-foot correction

c) 16-foot correction

d) 90˚ correction at 16 feet

Figure 7 Extrapolated windscreen corrections using airball source for the Kevar120 screen and the 32-inch electret array using Fleury-Horne method.



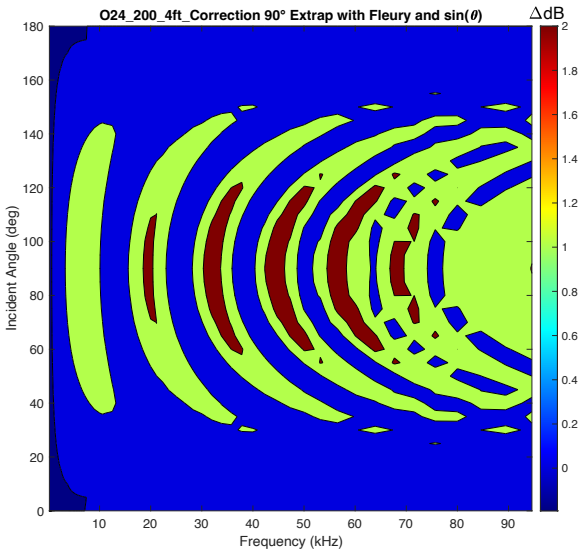
a) 4-foot correction

b) 8-foot correction

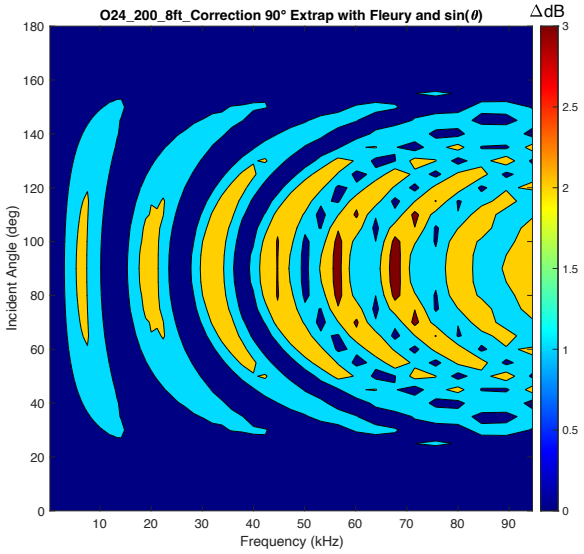
c) 16-foot correction

d) 90˚ correction at 8 feet

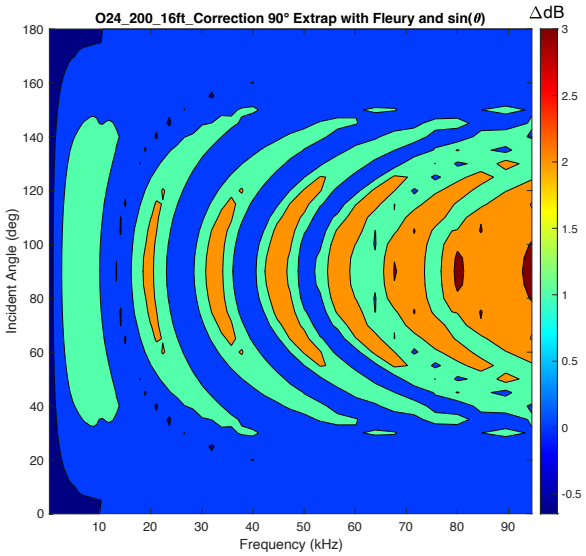
Figure 8 Extrapolated windscreen corrections for 8-inch I24 array with ss200x600 screen using airball source and the using Fleury-Horne method.



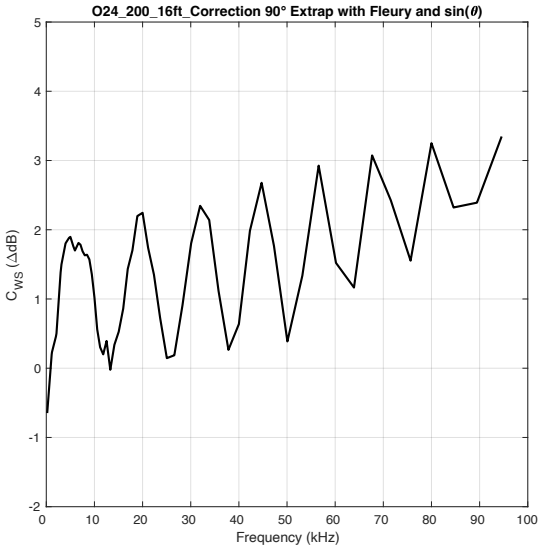
a) 4-foot correction



b) 8-foot correction

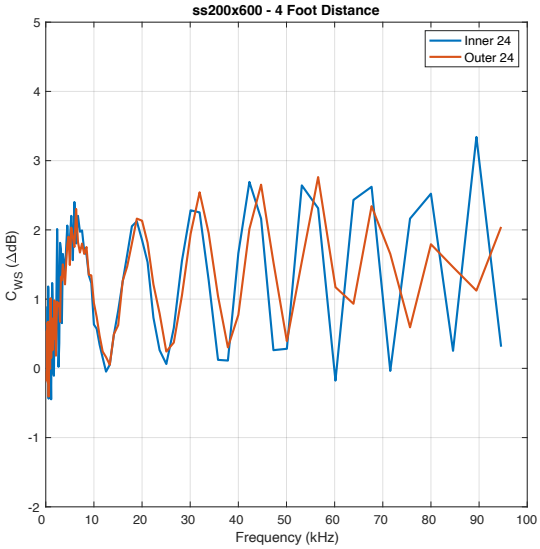


d) 16-foot correction

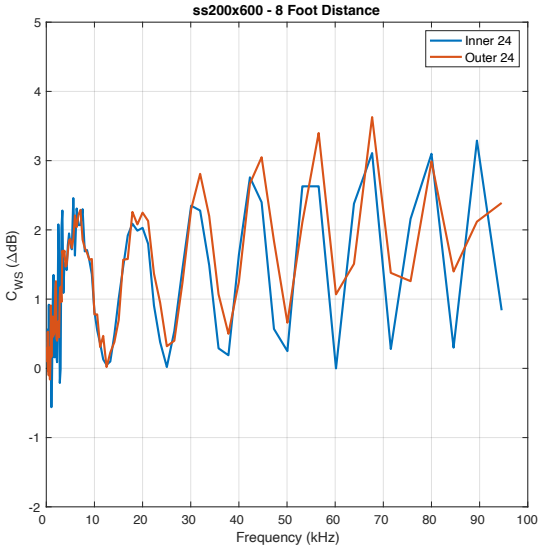


d) 90˚ correction at 16 feet

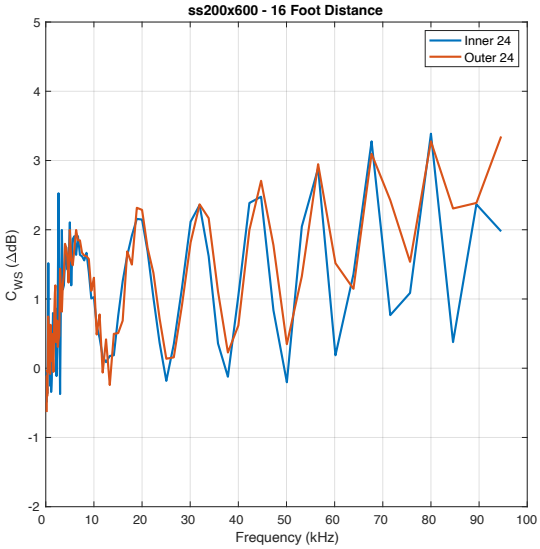
Figure 9 Extrapolated windscreen corrections for 23-inch O24 array with ss200x600 screen using airball source and the using Fleury-Horne method.



a) 4-foot correction

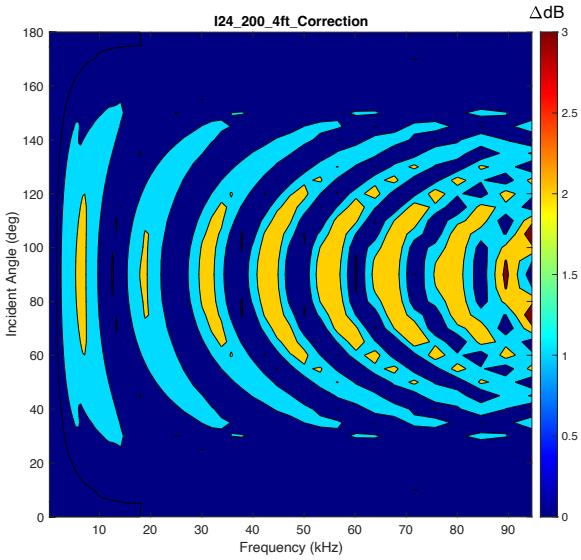


b) 8-foot correction

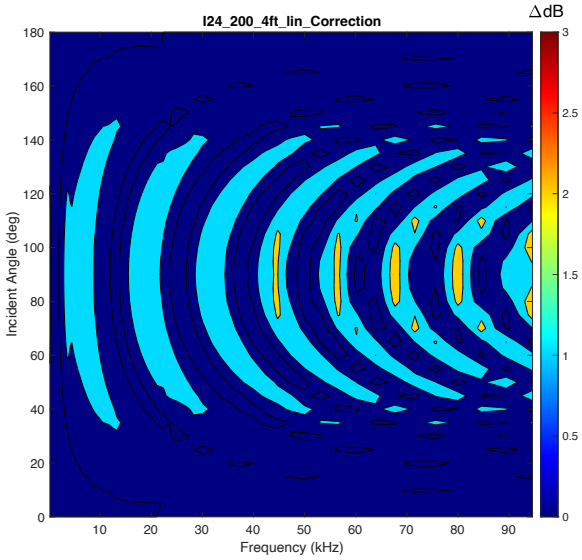


c) 16-foot correction

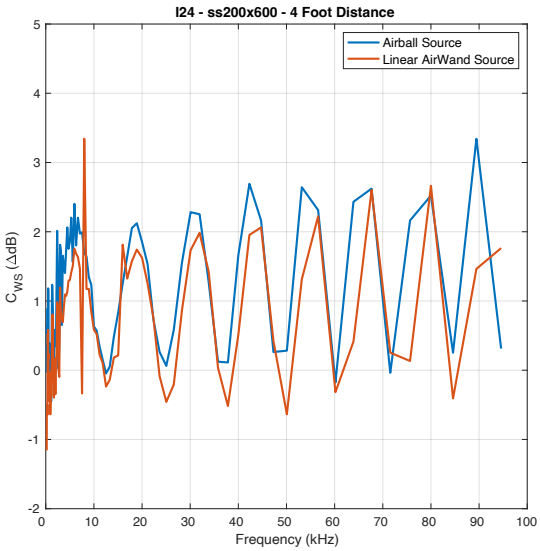
Figure 10 I24 and O24 ss200x600 windscreen corrections at 90°



a) compact airball source Cws

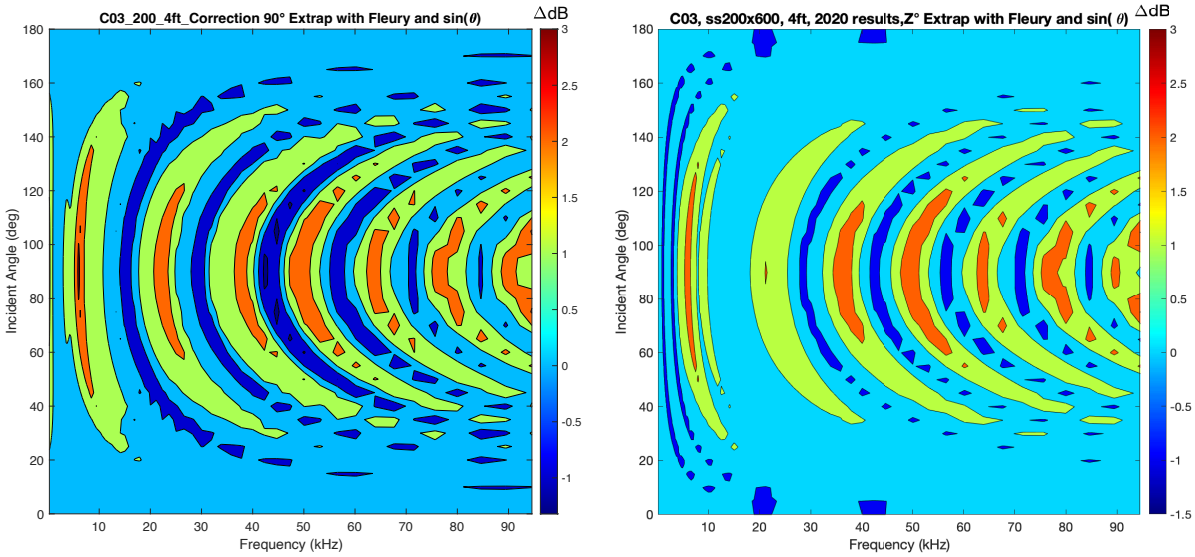


b) linear source Cws



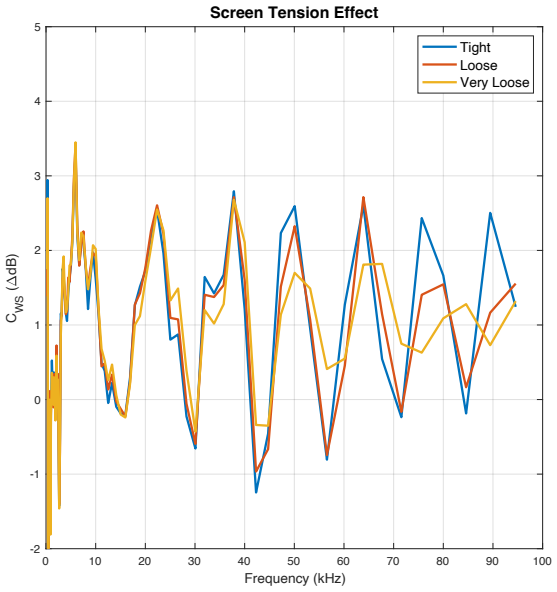
c) 90° comparison of sources

Figure 11 Comparison of 8-inch I24 ss200x600 screen corrections derived using airball compact pneumatic source and linear array of microjets.

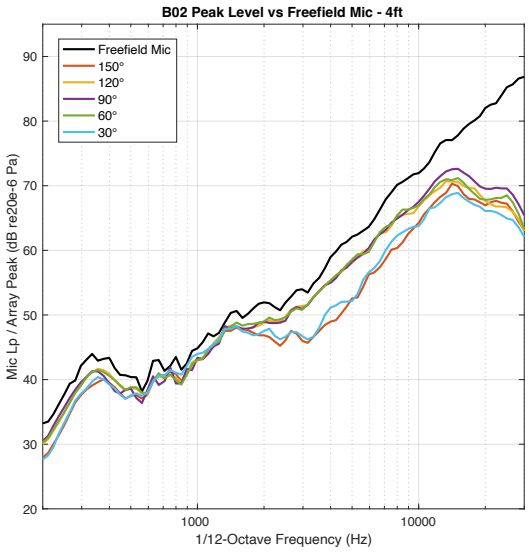


a) 2022 Calibration **b) 2020 Calibration**

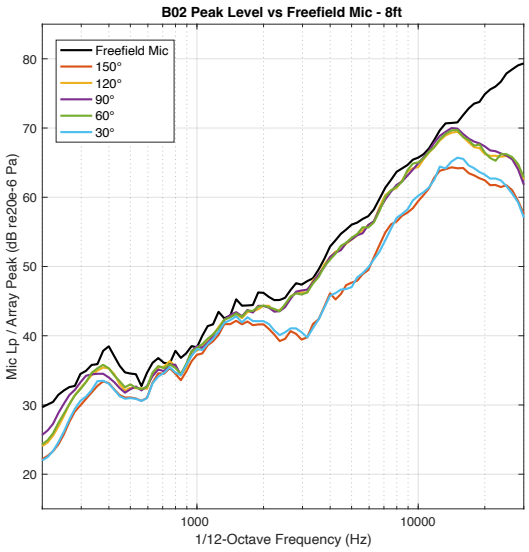
Figure 12 Comparison of Common Array (8-inch) windscreen corrections measured in 2022 and 2020. Windscreen corrections are extrapolated from 90˚ measurements for the ss200x600 screen using Fleury-Horne method.



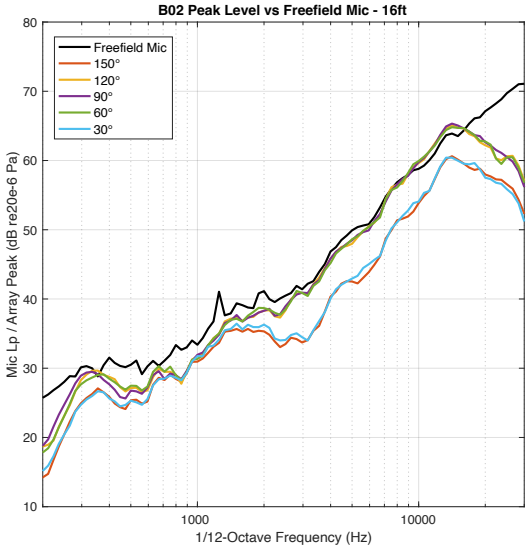
ommon Array.



a) 4-foot measurement

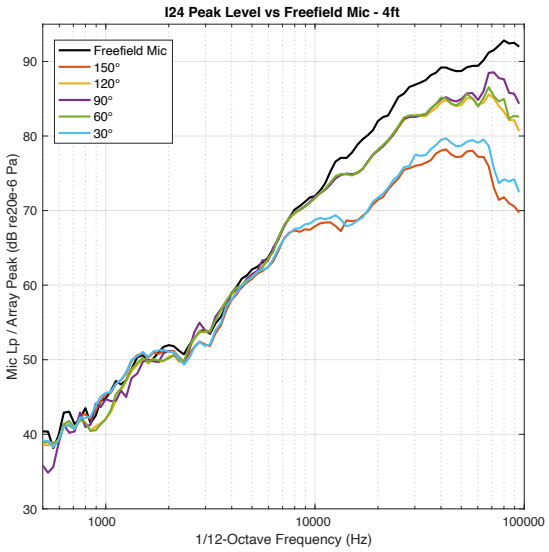


b) 8-foot measurement

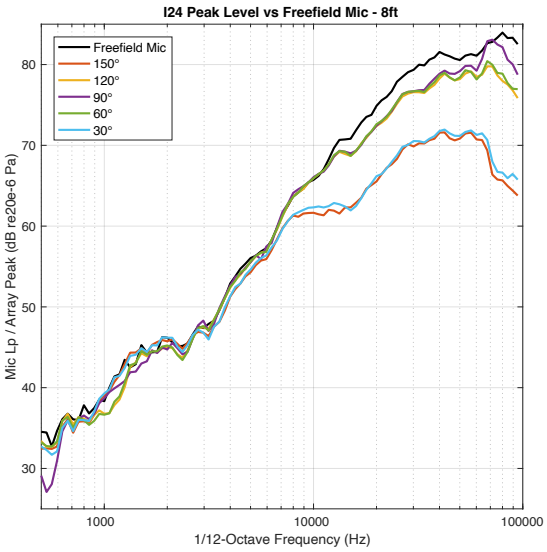


c) 16-foot measurement

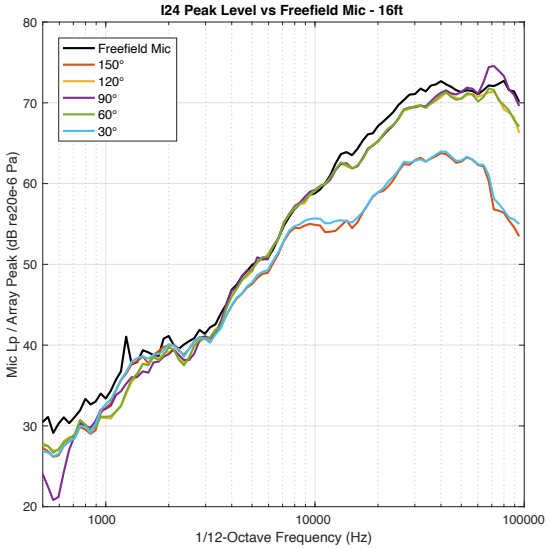
Figure 14 Comparison of 32-inch electret array peak levels and free-field single microphone measurements at 3 distances. Five incidence angles are plotted to show array accuracy.



a) 4-foot measurement

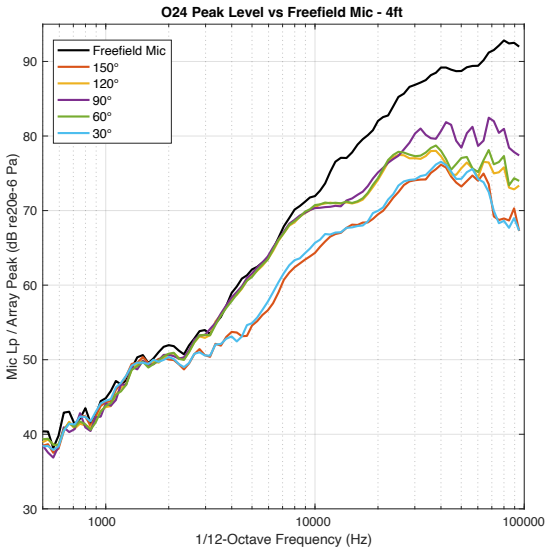


b) 8-foot measurement

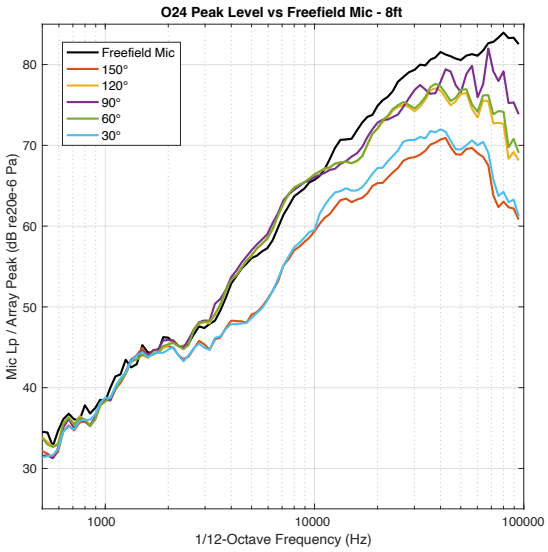


c) 16-foot measurement

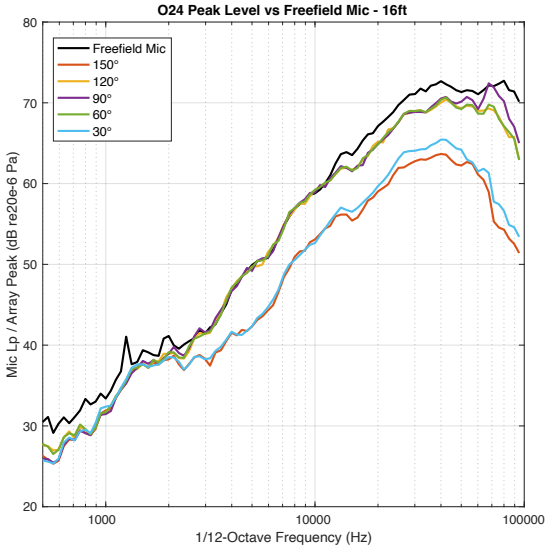
Figure 15 Comparison of 8-inch I24 array peak levels and free-field single microphone measurements at 3 distances. Five incidence angles are plotted to show array accuracy.



a) 4-foot measurement



b) 8-foot measurement



c) 16-foot measurement

Figure 16 Comparison of 23-inch O24 array peak levels and free-field single microphone measurements at 3 distances. Five incidence angles are plotted to show array accuracy.